Chemical Science

ROYAL SOCIETY OF CHEMISTRY

EDGE ARTICLE

View Article Online
View Journal | View Issue

Cite this: *Chem. Sci.*, 2021, **12**, 7569

All publication charges for this article have been paid for by the Royal Society of Chemistry

Received 18th February 2021
Accepted 12th April 2021

DOI: 10.1039/d1sc00988e

rsc.li/chemical-science

Anion mediated, tunable isoguanosine self-assemblies: decoding the conformation influence and solvent effects†‡

Mengjia Liu,[a] Ying He,[a] Chuan Shan,[a] Lukasz Wojtas,[a] Ion Ghiviriga,[c] Omar Fathalla,[a] Yu Yan,[a] Xiaopeng Li[ab] and Xiaodong Shi*[a]

Systematic investigations were performed with various substituted groups at C8 purine and ribose. A series of isoG analogs, C8-phenyl substituted isoG were synthesized and applied for Cs^+ coordination. The structural proximity between purine and ribose limited pentaplex formation for C8-phenyl substituted isoG derivatives. Based on this observation, deoxy isoG derivative with modification on ribose (*tert*-butyldimethylsilyl ether) was applied to assemble with the Cs^+ cation. Critical solvent ($CDCl_3$ and CD_3CN) and anion (BPh_4^-, $BARF^-$, and PF_6^-) effects were revealed, leading to the controllable formation of various stable isoG pentaplexes, including singly charged decamer, doubly charged decamer, and 15-mer, *etc.* Finally, the X-ray crystal structure of $[isoG_{20}Cs_3]^{3+}(BARF^-)_3$ was successfully obtained, which is the first example of multiple-layer deoxy isoG binding with the Cs^+ cation, providing solid evidence of this new isoG ionophore beyond two-layer sandwich self-assembly.

Introduction

The core value of supramolecular chemistry is the efficient construction of highly ordered structures at the molecular level through controllable building block interactions.[1] The fundamental scientific tasks in supramolecular chemistry are (A) to develop building blocks that could conduct efficient non-covalent interactions; (B) to understand the driving forces between molecules to reach controllable molecular architecture; and (C) to apply these systems as potential solutions for important scientific problems that are difficult and/or challenging when using alternative covalent approaches.[2] To reach these goals, development of basic supramolecular building blocks and understanding the driving forces toward the formation of specific non-covalent interactions are of great importance for tackling challenging scientific questions in alternative covalent approaches.[3]

Isoguanosine (isoG, also known as 2-hydroxy-adenosine) is a structural isomer of guanosine (G).[4] IsoG pentaplex is an interesting supramolecular scaffold with intrinsic H-bond donors and acceptors. The 108° H-bond angle allows isoG to form a larger self-assembled core beyond tetrameric structures

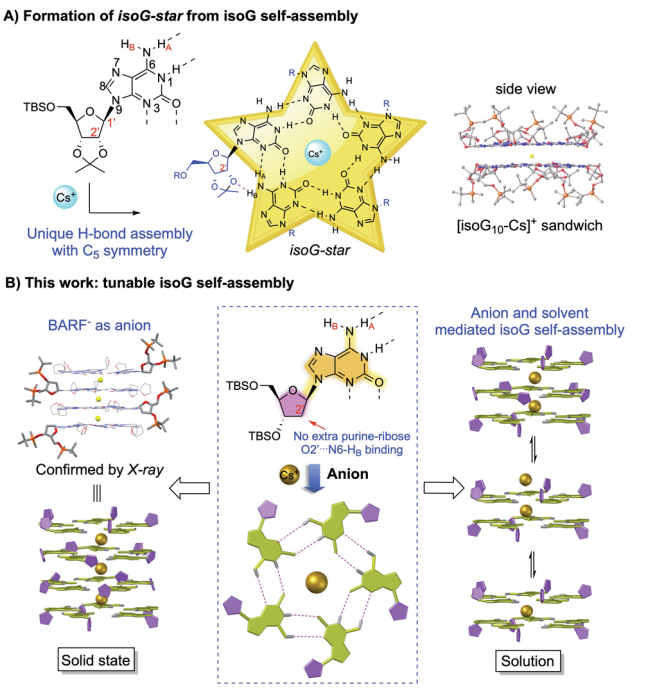

Scheme 1 IsoG self-assembly with unique C_5 symmetry. (A) Formation of *isoG-star* from isoG self-assembly; (B) tunable deoxy isoG self-assembly.

[a]*Department of Chemistry, University of South Florida, 4202 E. Fowler Avenue, Tampa, Florida 33620, USA. E-mail: xmshi@usf.edu*

[b]*College of Chemistry and Environmental Engineering, Shenzhen University, Shenzhen 518055, People's Republic of China*

[c]*Department of Chemistry, University of Florida, 125 Buckman Drive, Gainesville, Florida 32611, USA*

† Dedicated to the 100th anniversary of Chemistry at Nankai University.

‡ Electronic supplementary information (ESI) available: Experimental section, NMR spectra, ESI-MS spectra and crystallographic data. CCDC 2039733, 2039734 and 2073701. For ESI and crystallographic data in CIF or other electronic format see DOI: 10.1039/d1sc00988e

formed by guanosine (G_4).[5] In 2000, the Davis group reported the first two X-ray crystal structures that provided the evidence for the formation of the H-bonded $isoG_5$ (*isoG-star*) self-assembly.[6] As shown in Scheme 1, the *isoG-star* holds an overall planar structure, while the sp^3 configuration at the C1′ position gives a twisted conformation between ribose and purine, producing a well-defined bowl-shape assembly, which further led to the formation of a stable sandwiched structure of $isoG_{10}$.

Unlike the G_4-quartet (square planar geometry), the $isoG_5$ gives a star-shaped building block with C_5 symmetry and larger pore.[7] This unique feature of isoG has enabled it to selectively bind with large size cation Cs^+ (radii = 174 pm) in high affinity. The selective binding of Cs^+ over other alkali and alkali earth metal cations makes $isoG_5$ a potential host for effective caesium-137 extraction in radioactive waste treatment.[8] However, little progress has been made in isoG self-assembly studies since the initial breakthrough.[9] This is probably due to the close distance between N9-ribose and N3-purine. Unlike G-quartet, where N3 is not involved in the H-bonding network, the N3 position is crucial in the isoG self-assembly as a key H-bond receptor. In addition, the crystal structure of *isoG-star* revealed interesting "extra H-bonds" between the ribose O2′ and purine N6-H_B (Scheme 1A). The purine–ribose interaction in the isoG pentamer makes it much more challenging for precise conformation control. Thus, new systems that could achieve isoG self-assembly with good stability and structural diversity are highly desirable. Herein, we report a systematic study of the influence of the isoG C8 substitution and ribose modification on the formation of *isoG-star*. Conditions to achieve controllable $isoG_5$ pentaplex have been investigated, which revealed the critical solvent and anion effects (Scheme 1B).[10] The successful preparation of singly charged decamer, doubly charged decamer and pentaplex $isoG_{15}$ through the anion and ribose conformation control was undoubtedly characterized by ^{1}H NMR, diffusion NMR and ESI-MS. The X-ray crystal structure of $[isoG_{20}Cs_3]^{3+}(\text{-BARF}^-)_3$ was successfully obtained, confirming the formation of pentaplex $isoG_{20}$ beyond the previously reported sandwich structure. These results not only highlighted the critical solvent and anion effects in this supramolecular assembly, but also provided new isoG-based structural motifs for molecular recognition and related potential applications.[11]

Results and discussion

As reported by Davis, isoG **1** has been used to react with $CsBPh_4$ for the formation of *isoG-star* (Fig. 1). The relatively rigid ribose modification successfully controlled the formation of a well-defined bowl-shaped structure, which led to the sandwiched $isoG_{10}$. Notably, as an H-bond receptor, the N3 position is crucial for the *isoG-star* formation. However, the structural proximity between N3 and ribose limited the choice of modification on ribose or purine. In addition, the crystal structure of *isoG-star* from isoG **1** revealed interesting "extra H-bonds" between the ribose O2′ and purine N6-H_B, which makes one wonder if this purine–ribose interaction is necessary for the stable *isoG-star* formation. With all these structural analyses, the purine C8 position is the ideal synthetic handle to introduce

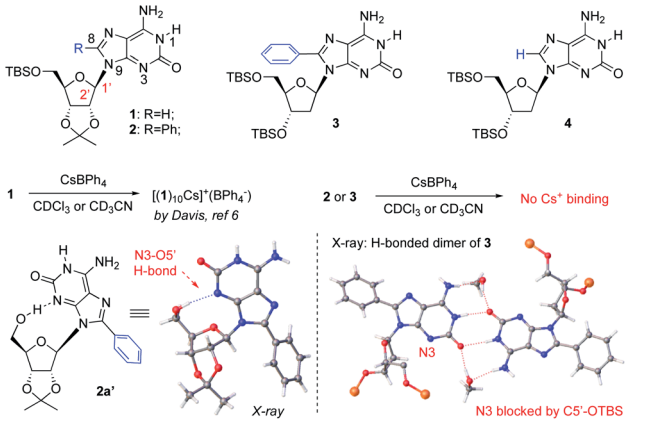

Fig. 1 Challenge of *isoG-star* formation using isoG derivatives.

new functionality without interrupting the needed H-bond in the *isoG-star* formation. The 8-phenyl modified compound isoG **2** was synthesized (see detailed synthesis in the ESI‡). To evaluate the importance of purine–ribose O2′···N6-H_B binding, 2-deoxy isoG **3** and **4** were also prepared. All these new isoG derivatives were applied in the self-assembly studies. It is known that, with the large cation radii, Cs^+ provides the best match toward the $isoG_5$ pore. As reported previously, treating isoG **1** in $CDCl_3$ solution with $CsBPh_4$ (aqueous solution) gave effective extraction of Cs^+ into the organic layer, forming stable $[(\mathbf{1})_{10}Cs]^+(BPh_4^-)$ complexes.[12] However, conducting similar experiments with isoG **2** or isoG **3** gave no formation of Cs^+ complexes.

Fortunately, the X-ray single crystal structures of both compounds were successfully obtained (Fig. 1). As shown in the crystal structures of isoG **2′** (from 5′-TBS-deprotection of **2**), the conformation of the free-rotatable C–N bond is influenced by substitution of the purine C8 position. The *anti*-conformation is energetically favored by avoiding steric repulsion. As a result, O5′ was placed close to N3, blocking critical H-bonding in the $isoG_5$ formation. With the less rigid deoxy-ribose with no O2′, isoG **3** gave a H-bonding dimer since N3 is not accessible for H-bonding, which is critical for the *isoG-star* formation. These results highlighted the challenge associated with developing new systems for the preparation of *isoG-star* from small molecular assembly. As revealed by the crystal structures, C8 functionalization prevents N3 from being accessible for H-bonding to form *isoG-star*.

To examine whether O2′···N6-H_B H-bonding is necessary for the stable *isoG-star* formation, deoxy-isoG **4** with no C8 phenyl group and O2′ was applied for self-assembly with Cs^+. As shown in Fig. 2E, treating isoG **4** with $CsBPh_4$ (excess amount) led to the formation of multiple sets of new signals in the ^{1}H NMR spectrum which indicated the formation of H-bonded complexes. Interestingly, monitoring the reaction over time suggested the formation of one major set of signals when treating the ligand and the cation for 30 minutes (Fig. 2D). The ^{1}H NMR spectrum integration confirmed that the ratio between isoG **4** and Cs^+ is 10 : 1. This result is exciting since it suggested the formation of *isoG-star* could be achieved with deoxy-isoG

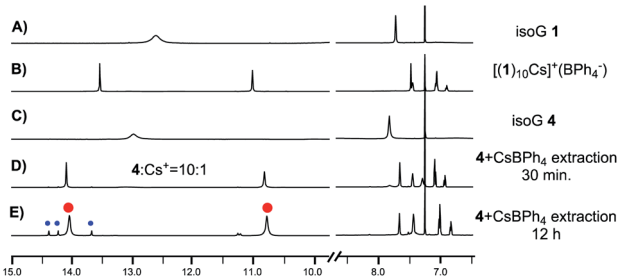

Fig. 2 ^{1}H NMR spectra showing formation of isoG monomers and complexes in $CDCl_3$ (A) isoG **1** monomer; (B) $[(\mathbf{1})_{10}Cs]^+(BPh_4^-)$; (C) isoG **4** monomer; (D) treating isoG **4** with $CsBPh_4$ for 30 min; (E) treating isoG **4** with $CsBPh_4$ for 12 h.

without the extra ribose–purine H-bond. Various conditions were used to obtain X-ray crystal structures. Fortunately, by switching the anion to $BARF^-$, a stable complex was obtained in a $CHCl_3$–CH_3CN solvent mixture with structure confirmed by X-ray crystallography as $[(\mathbf{4})_{20}Cs_3]^{3+}(BARF^-)_3$ (Fig. 3). Notably, this is not only the first crystal structure of an isoG-assembly from deoxy-ribose but also the first multiple-layer isoG pentaplex beyond the sandwich structure reported so far.

As shown in the crystal structure, the $isoG_{20}$ assembly was formed with the deoxy-ribose ligand. The Cs^+ cations bind to $isoG_5$ between layers through ion–dipole interactions, similar to the previously reported $isoG_{10}$ from isoG **1**. The H-bond distance between N1–O2 is 2.71 ± 0.03 Å and N6–N3 is 2.88 ± 0.03 Å, similar to the H-bond distance observed in $[(\mathbf{1})_{10}Cs]^+$. The distances between $isoG_5$ layers in $[(\mathbf{4})_{20}Cs_3]^{3+}(BARF^-)_3$ are between 3.20 and 3.37 Å, almost identical to the distance observed in the isoG **1** complex, suggesting similar ion–dipole interactions in this deoxy-isoG complexes. The biggest difference between these two types of isoG-assemblies is the ribose conformation. In $[(\mathbf{1})_{10}Cs]^+(BPh_4^-)$, the two $isoG_5$ pentamers stack in a tail-to-tail configuration. With more flexible deoxy ribose, $isoG_5$ from isoG **4** is less sterically hindered, allowing ribose side chain interdigitation between layers. As shown in complex $[(\mathbf{1})_{10}Cs]^+$, the opposite H-bond orientation is crucial for the formation of strong ion–dipole interactions (Cs^+ to O2). Similar stacking pattern was observed in $[(\mathbf{4})_{20}Cs_3]^{3+}(BARF^-)_3$, where the reversed H-bond orientation was observed between two adjacent layers, giving either a head-to-head or tail-to-tail configuration throughout the structures. This result is important since it revealed the possibility to further extend the structure along the *c*-axis with this new deoxy-ribose isoG for potential applications, such as the Cs^+ ion-channel.

With the solid-state structure confirmed by X-ray crystallography, we then focused on the self-assembly in the solution. As discussed above, since this deoxy *isoG-star* could further extend the assembly along the vertical direction, achieving a controllable pentaplex is critical for potential future applications. To study how deoxy-isoG **4** binds with Cs^+ in solution, we first dissolved $[(\mathbf{4})_{20}Cs_3]^{3+}(BARF^-)_3$ in $CDCl_3$ and monitored by ^{1}H NMR. As shown in Fig. 4A, dissolving $[(\mathbf{4})_{20}Cs_3]^{3+}(BARF^-)_3$ in $CDCl_3$ gave a mixture of various H-bonded complexes (see full spectra in Fig. S2‡). To identify the structures of these complexes, we conducted a series of titration experiments based on ^{1}H NMR.

First, unlike the BPh_4^- anion (Fig. 2E), treating isoG **4** with excess of CsBARF gives the formation of a complex with 5 : 1 ratio between isoG **4** and Cs^+ (Fig. 4B). Notably, treating isoG **4** with limited amount of Cs^+ could form $[(\mathbf{4})_{10}Cs]^+$ (Fig. 4D). Interestingly, titration experiments (addition of isoG **4** into the 5 : 1 complex) revealed the formation a new complex with three sets of NMR signals in 1 : 1 : 1 ratio (complex **A**, Fig. 4C). To

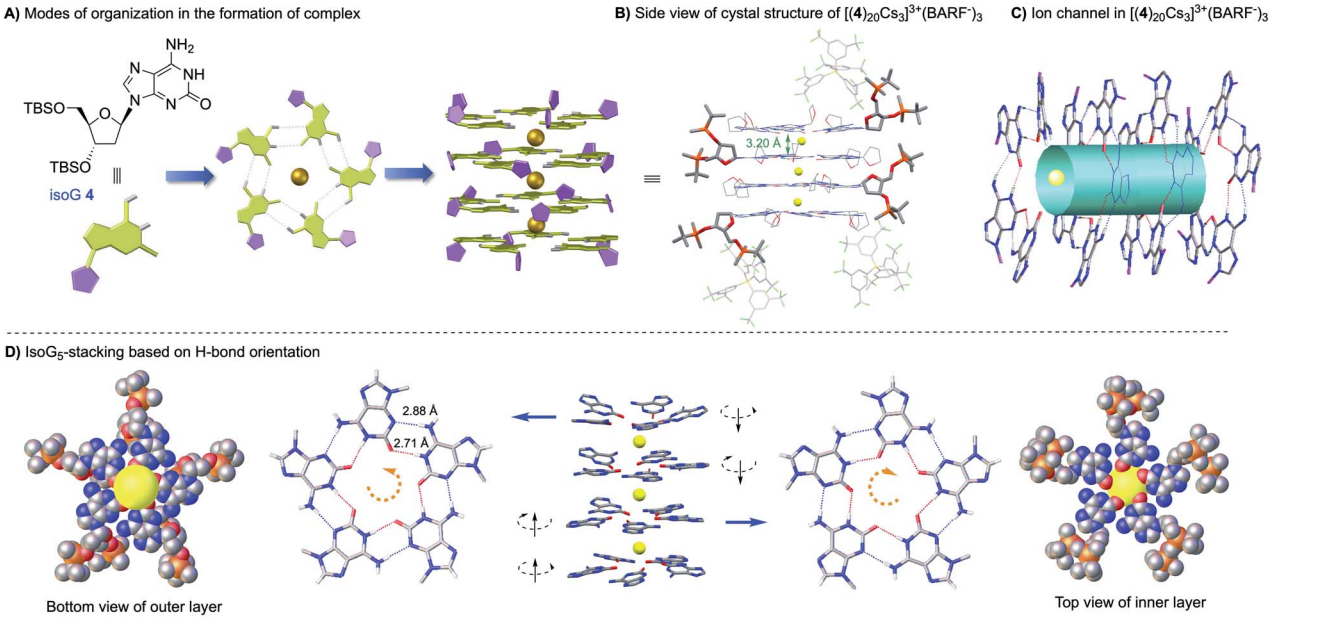

Fig. 3 X-ray single crystal structure of the deoxy $isoG_{20}$, (A) modes of organization in the formation of the complex; (B) side view of $[(\mathbf{4})_{20}Cs_3]^{3+}(BARF^-)_3$; (C) ion channel in $[(\mathbf{4})_{20}Cs_3]^{3+}(BARF^-)_3$; (D) outer and inner layer.

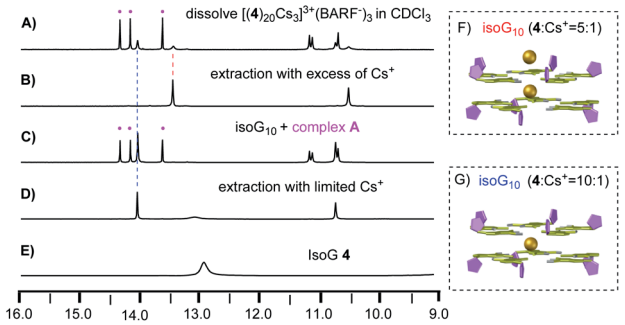

Fig. 4 ^{1}H NMR spectra of isoG **4** assemblies in $CDCl_3$ (A) dissolving $[(\mathbf{4})_{20}Cs_3]^{3+}(BARF^-)_3$ crystal in $CDCl_3$; (B) adding excess of Cs^+ in solution; (C) adding isoG **4** in solution B; (D) 10 : 1 ratio of isoG **4** : Cs^+ in solution; (E) no cation added; (F) model of doubly charged decamer formed; (G) model of singly charged decamer formed.

elucidate the composition of the stable 5 : 1 complex as $[(\mathbf{4})_5Cs]^+$ or $[(\mathbf{4})_{10}Cs_2]^{2+}$, diffusion ordered spectroscopy (DOSY) experiments were performed (see the ESI‡), which was firstly reported by Cohen.[12] The diffusion coefficients of ribose H1′ were determined as $2.87 \pm 0.02 \times 10^{-10}$ m^2 s^{-1} (5 : 1 complex) and $3.37 \pm 0.01 \times 10^{-10}$ m^2 s^{-1} (10 : 1 complex) (Fig. S7 and S8‡). These results strongly suggested the formation of $[(\mathbf{4})_{10}Cs_2]^{2+}$ instead of $[(\mathbf{4})_5Cs]^+$. To further confirm this composition analysis, direct comparisons between 5 : 1 and 10 : 1 complexes formed from deoxy isoG **4** and isopropylidene isoG **1** were performed. The diffusion coefficients of these four complexes are summarized in Table S1.‡ The diffusion coefficient values of H1′ were observed for the 5 : 1 complex from isoG**1** as $3.11 \pm 0.06 \times 10^{-10}$ m^2 s^{-1} and the 10 : 1 complex as $3.33 \pm 0.09 \times 10^{-10}$ m^2 s^{-1}. These results strongly suggested the formation of $[(\mathbf{1})_{10}Cs_2]^{2+}$ with the $BARF^-$ anion in $CDCl_3$ solution, which further confirmed the formation of $[(\mathbf{4})_{10}Cs_2]^{2+}$ as described above.

It has been previously reported that treating isoG **1** with excess $CsBPh_4$ gave $[(\mathbf{1})_{10}Cs]^+$ (Fig. 5B). A similar decamer assembly was formed with the PF_6^- anion (Fig. 5C). As described above, switching the anion to $BARF^-$ gives the formation of a new set of signals (Fig. 5A), suggesting the special anion effect of $BARF^-$. Comparing ^{1}H NMR spectra of $[(\mathbf{4})_{10}Cs_2]^{2+}(BARF^-)_2$ with free $BARF^-$ solution (cryptand complex, Fig. 5G), different chemical shifts were observed, indicating the interaction of the $BARF^-$ anion toward the pentaplex in solution (Fig. 5H), which was further confirmed by the diffusion coefficients of $BARF^-$ (see Fig. S7 and S8‡).

With the ability to control the formation of singly charged decamer and doubly charged decamer, we turned our attention to determine the structure of complex **A**. Considering that the solid-state stable $[(\mathbf{4})_{20}Cs_3]^{3+}(BARF^-)_3$ was observed from evaporation of $CHCl_3$ and CH_3CN mix solvents, we hypothesized that the polarity difference of solvents could be crucial for the formation of complex **A**. Notably, the Meijer group reported the G-quadruplex self-assembly controlled by the coulombic interaction. The authors suggested that the ion pair separation could be regulated through tuning solvent polarity.[13] Inspired by this

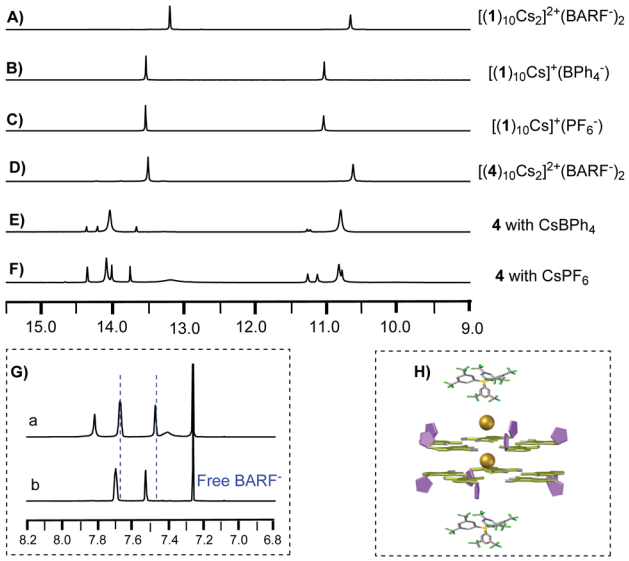

Fig. 5 Critical anion-effect in the *isoG-star* coordination with the Cs^+ cation (A) $[(\mathbf{1})_{10}Cs_2]^{2+}(BARF^-)_2$; (B) $[(\mathbf{1})_{10}Cs]^+(BPh_4^-)$; (C) $[(\mathbf{1})_{10}Cs]^+(PF_6^-)$; (D) $[(\mathbf{4})_{10}Cs_2]^{2+}(BARF^-)_2$; (E) treating **4** with $CsBPh_4$; (F) treating **4** with $CsPF_6$. (G) ^{1}H NMR spectra of (a) $[(\mathbf{4})_{10}Cs_2]^{2+}(BARF^-)_2$ and (b) free $BARF^-$ solution (cryptand complex); (H) model of the doubly charged decamer formed.

work, polar solvent (like CH_3CN) would cause the dissociation of the ion-pair between *isoG-star* and the $BARF^-$ anion. Therefore, tuning the polarity of solvents might be critical to reach the optimal conditions for the formation of complex **A**. Solvent titration was performed using a mixture of $CDCl_3$ and CD_3CN. The self-assembly process was monitored by ^{1}H NMR (Fig. 6).

In less polar $CDCl_3$, doubly charged decamer was formed (Fig. 6A). Addition of CD_3CN caused increase in polarity with gradual formation of complex **A**. Finally, in the 1 : 1 mixture of $CDCl_3$ and CD_3CN, complex **A** was achieved as the dominant structure. ^{1}H NMR spectra integration confirmed the proposed $[(\mathbf{4})_{15}Cs_2]^{2+}(BARF^-)_2$, consistent with the observed three set of signals (Fig. 6G). In addition, this structure was further confirmed using ESI-MS, giving the doubly charged peak with

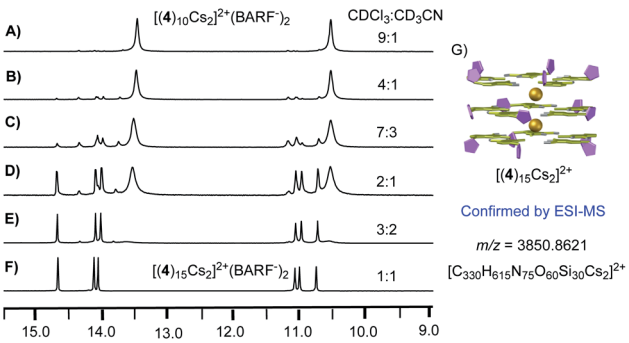

Fig. 6 ^{1}H NMR spectra of CD_3CN titration experiments using $[(\mathbf{4})_{10}Cs_2]^{2+}(BARF^-)_2$ (A) $CDCl_3$: CD_3CN = 9 : 1; (B) $CDCl_3$: CD_3CN = 4 : 1; (C) $CDCl_3$: CD_3CN = 7 : 3; (D) $CDCl_3$: CD_3CN = 2 : 1; (E) $CDCl_3$: CD_3CN = 3 : 2; (F) $CDCl_3$: CD_3CN = 1 : 1; (G) model of $isoG_{15}$ formed.

m/*z* at 3850.8621 (Fig. S6‡). These experiments confirmed that the more polar solvents which can separate ion pairs favor the formation of larger assemblies. Notably, conducting the similar reaction with isoG **1**, gave discrete $isoG_{10}$ decamer in CD_3CN with no formation of multiple-layer pentaplex, which highlighted the versatile coordination ability of deoxy-isoG **4** in the formation of pentaplex and critical solvent effect in the isoG self-assembly process.

Conclusions

In conclusion, influence of the purine C8 position and ribose functionalization in the isoG derivative self-assembly with the Cs^+ cation was explored. Although C8 substituents prevent N3 from being accessible for H-bonding formation in the *isoG-star*, we successfully discovered that 2′-deoxy isoG with no O2′ could serve as a new building block to achieve controllable supramolecular assemblies. This finding suggests that O2′···N6-H_B H-bonding is not necessary for the stable *isoG-star* formation. Based on the coordination with the $BARF^-$ anion and solvent mixtures, complexes such as $isoG_{10}$, $isoG_{15}$, and $isoG_{20}$ were achieved with structures characterized by ^1H NMR, diffusion NMR, ESI-MS and X-ray crystallography. This study not only revealed the important anion and solvent effects in the formation of various isoG self-assemblies, but also paved the crucial foundation for the *isoG-star* as a new scaffold in molecular architecture for future applications.

Author contributions

X. S. conceived the original idea and research direction and supervised the research. X. S. and M. L. designed the study. M. L. carried out the material synthesis and characterization; M. L. and Y. H. analyzed the results and data; C. S. and W. L. performed the X-ray measurements and analyzed the data; Y. Y. and X. L. contributed to the ESI-MS; I. G. performed the DOSY experiments. All authors discussed and commented on the manuscript.

Conflicts of interest

There are no conflicts to declare.

Acknowledgements

We are grateful to the NSF (CHE-1665122) and NIH (1R01GM120240-01) for financial support. This work was supported in part by the University of South Florida Interdisciplinary NMR Facility and the Chemical Purification, Analysis, and Screening (CPAS) Core Facility.

Notes and references

1 (*a*) L. J. Prins, F. De Jong, P. Timmerman and D. N. Reinhoudt, *Nature*, 2000, **408**, 181–184; (*b*) L. J. Prins, D. N. Reinhoudt and P. Timmerman, *Angew. Chem., Int. Ed.*, 2001, **40**, 2382–2426; (*c*) M. M. Safont-Sempere, G. Fernández and F. Würthner, *Chem. Rev.*, 2011, **111**, 5784–5814; (*d*) A. Pal, M. Malakoutikhah, G. Leonetti, M. Tezcan, M. Colomb-Delsuc, V. D. Nguyen, J. van der Gucht and S. Otto, *Angew. Chem., Int. Ed.*, 2015, **54**, 7852–7856; (*e*) M. Zeraati, D. B. Langley, P. Schofield, A. L. Moye, R. Rouet, W. E. Hughes, T. M. Bryan, M. E. Dinger and D. Christ, *Nat. Chem.*, 2018, **10**, 631–637.

2 (*a*) J. Murray, K. Kim, T. Ogoshi, W. Yao and B. C. Gibb, *Chem. Soc. Rev.*, 2017, **46**, 2479–2496; (*b*) G. Vantomme and E. W. Meijer, *Science*, 2019, **363**, 1396–1397; (*c*) W. R. Henderson, Y. Zhu, D. E. Fagnani, G. Liu, K. A. Abboud and R. K. Castellano, *J. Org. Chem.*, 2020, **85**, 1158–1167.

3 (*a*) M. García-Arriaga, G. Hobley and J. M. Rivera, *J. Am. Chem. Soc.*, 2008, **130**, 10492–10493; (*b*) D. E. Fagnani, M. J. Meese Jr, K. A. Abboud and R. K. Castellano, *Angew. Chem., Int. Ed.*, 2016, **55**, 10726–10731; (*c*) J. Lu, I. Hung, A. Brinkmann, Z. Gan, X. Kong and G. Wu, *Angew. Chem., Int. Ed.*, 2017, **129**, 6262–6266; (*d*) Y. He, Y. Zhang, L. Wojtas, N. G. Akhmedov, D. Thai, H. Wang, X. Li, H. Guo and X. Shi, *Chem. Sci.*, 2019, **10**, 4192–4199; (*e*) Y. Liu, W. Zhao, C.-H. Chen and A. H. Flood, *Science*, 2019, **365**, 159–161; (*f*) W. Zhao, J. Tropp, B. Qiao, M. Pink, J. D. Azoulay and A. H. Flood, *J. Am. Chem. Soc.*, 2020, **142**, 2579–2591.

4 (*a*) F. Fuhrman, G. Fuhrman, R. Nachman and H. Mosher, *Science*, 1981, **212**, 557–558; (*b*) J. T. Davis and G. P. Spada, *Chem. Soc. Rev.*, 2007, **36**, 296–313; (*c*) D. Jiang and F. Seela, *J. Am. Chem. Soc.*, 2010, **132**, 4016–4024; (*d*) Q. Cheng, J. Gu, K. R. Compaan and H. F. Schaefer III, *Chem.–Eur. J.*, 2012, **18**, 4877–4886; (*e*) S. A. Ingale, P. Leonard, Q. N. Tran and F. Seela, *J. Org. Chem.*, 2015, **80**, 3124–3138; (*f*) H. Zhao, H. Feng, J. Liu, F. Tang, Y. Du, N. Ji, L. Xie, X. Zhao, Z. Wang and Q. Chen, *Biomaterials*, 2020, **230**, 119598.

5 (*a*) M. Cai, X. Shi, V. Sidorov, D. Fabris, Y.-f. Lam and J. T. Davis, *Tetrahedron*, 2002, **58**, 661–671; (*b*) J. T. Davis, *Angew. Chem., Int. Ed.*, 2004, **43**, 668–698; (*c*) T. Ding, F. Tang, G. Ni, J. Liu, H. Zhao and Q. Chen, *RSC Adv.*, 2020, **10**, 6223–6248.

6 (*a*) X. Shi, J. C. Fettinger, M. Cai and J. T. Davis, *Angew. Chem., Int. Ed.*, 2000, **39**, 3124–3127; (*b*) M. M. Cai, A. L. Marlow, J. C. Fettinger, D. Fabris, T. J. Haverlock, B. A. Moyer and J. T. Davis, *Angew. Chem., Int. Ed.*, 2000, **112**, 1339–1341.

7 (*a*) C. Zhong, J. Wang, N. Wu, G. Wu, P. Y. Zavalij and X. Shi, *Chem. Commun.*, 2007, 3148–3150; (*b*) V. Abet, R. Evans, F. Guibbal, S. Caldarelli and R. Rodriguez, *Angew. Chem., Int. Ed.*, 2014, **53**, 4862–4866; (*c*) H. Zhao, A. H. Schäfer and F. Seela, *ChemPlusChem*, 2017, **82**, 826–833; (*d*) F. Tang, H. Feng, Y. Du, Y. Xiao, H. Dan, H. Zhao and Q. Chen, *Chem.–Asian J.*, 2018, **13**, 1962–1971; (*e*) Y. He, Y. Zhang, L. Wojtas, N. G. Akhmedov, Q. Pan, H. Guo and X. Shi, *Chem.–Asian J.*, 2020, **15**, 1030–1034.

8 (*a*) S. C. Lee, J. D. Lamb, M. Cai and J. T. Davis, *J. Inclusion Phenom. Macrocyclic Chem.*, 2001, **40**, 51–57; (*b*) Z. Zhang, K. Ninomiya, Y. Yamaguchi, K. Kita, H. Tsuruta, Y. Igarashi

and A. Shinohara, *Environ. Sci. Technol.*, 2018, **52**, 9917–9925; (*c*) M. A. Olatunji, M. U. Khandaker, E. H. N. M. Mahmud, Y. M. Amin, J. A. Ademola and D. O. Olorode, *J. Radioanal. Nucl. Chem.*, 2018, **316**, 933–945; (*d*) F. W. Van Leeuwen, W. Verboom, X. Shi, J. T. Davis and D. N. Reinhoudt, *J. Am. Chem. Soc.*, 2004, **126**, 16575–16581; (*e*) F. W. van Leeuwen, J. T. Davis, W. Verboom and D. N. Reinhoudt, *Inorg. Chim. Acta*, 2006, **359**, 1779–1785.

9 (*a*) M. Meyer and J. Sühnel, *J. Phys. Chem. A*, 2003, **107**, 1025–1031; (*b*) J. Gu, J. Wang and J. Leszczynski, *J. Comput. Chem.*, 2007, **28**, 1790–1795; (*c*) J. Gu, J. Wang and J. Leszczynski, *Chem. Phys. Lett.*, 2007, **445**, 243–245.

10 (*a*) J. E. Betancourt, M. Martín-Hidalgo, V. Gubala and J. M. Rivera, *J. Am. Chem. Soc.*, 2009, **131**, 3186–3188; (*b*) E. Fadaei, M. Martín-Arroyo, M. Tafazzoli and D. González-Rodríguez, *Org. Lett.*, 2017, **19**, 460–463; (*c*) M. Martín-Arroyo, A. del Prado, R. Chamorro, N. Bilbao and D. González-Rodríguez, *Angew. Chem., Int. Ed.*, 2020, **59**, 9041–9046.

11 (*a*) S. Tirumala and J. T. Davis, *J. Am. Chem. Soc.*, 1997, **119**, 2769–2776; (*b*) P. Xin, P. Zhu, P. Su, J.-L. Hou and Z.-T. Li, *J. Am. Chem. Soc.*, 2014, **136**, 13078–13081; (*c*) R. N. Das, Y. P. Kumar, O. M. Schütte, C. Steinem and J. Dash, *J. Am. Chem. Soc.*, 2015, **137**, 34–37.

12 T. Evan-Salem, L. Frish, F. W. van Leeuwen, D. N. Reinhoudt, W. Verboom, M. S. Kaucher, J. T. Davis and Y. Cohen, *Chem.–Eur. J.*, 2007, **13**, 1969–1977.

13 D. González-Rodríguez, J. L. J. van Dongen, M. Lutz, A. L. Spek, A. P. H. J. Schenning and E. W. Meijer, *Nat. Chem.*, 2009, **1**, 151–155.